Nanostructured thin films by self-assembly of surface modified colloidal particles

Murali Sastry

Materials Chemistry Division, National Chemical Laboratory, Pune 411 008, India

The organization of nanoparticles in thin film form is an important element en route to commercially harnessing the exciting application potential of nanoscale matter. Self-assembly of nanoparticles synthesized by the colloidal route on suitable supports is one of the interesting techniques currently being investigated for realizing such structures. This article attempts to cover recent developments in this area with particular emphasis on the methodology developed in this laboratory for the growth of thin films of colloidal nanoparticles. Some other interesting issues related to application of surface-modified colloidal particles will also be addressed.

AS we enter the new millennium, Feynman's prophesy that miniaturization would play a key role in future technologies appears to be coming true due to important advances in the area of nanoscience[1]. This is a combination of many factors, not the least of which is due to the exciting developments in the area of self-assembly of nanoscale objects into ordered structures. While the novel physicochemical and optoelectronic properties of nanoparticles are well-known and understood[2,3], commercial application of nanoparticles would require their organization in thin film form with effective packaging. This article attempts to cover some of the recent developments in this so-called 'bottom-up' approach to nanoscale architecture[4], with bias towards work emanating from my lab. Some digression to illustrate interesting applications of surface-modified colloidal particles (which, in some ways, is the most important step in this bottom-up approach) will hopefully be pardoned.

The bottom-up method for forming thin films of nanoparticles consists essentially of two steps. The first step involves the synthesis of the nanoparticles by different processes and is followed by self-assembly of the nanoparticles on suitable substrates to yield thin films. The colloidal route for the synthesis of nanoparticles is particularly attractive for the bottom-up methodology for a number of reasons. Nanoparticles over a range of compositions and sizes with good control over the monodispersity of the particle size distribution (PSD) can be easily grown by the colloidal method. Another advantage of the colloidal route is that surface-modification of the nanoparticles may be achieved by solution-based self-assembly of suitable surfactants. As mentioned earlier, surface-modification (the term surface-derivatization is often used interchangeably with surface-modification in the literature) of colloidal particles is a key ingredient in the bottom-up recipe, has exciting application potential and will therefore be dealt with in some detail here. Since this paper deals with the self-assembly of nanoparticles synthesized by the colloidal route, the terms 'colloidal particle' and 'nanoparticle' will be used interchangeably. This is not strictly correct in all cases and must be borne in mind.

e-mail: sastry@ems.ncl.res.in

Surface-modification of nanoparticles

Brust and co-workers[5] demonstrated for the first time that alkanethiols spontaneously self-assemble on colloidal gold particles. The process of capping of colloidal particles with surfactants has come to be called 3-D self-assembly to differentiate between the more thoroughly studied 2-D self-assembly of alkanethiols on gold[6,7]/ alkylsilanes on silica[8,9] surfaces. A strong thiolate bond between the surfactant and the gold surface (this approach works equally well with silver and CdS nanoparticles) drives the self-assembly of the surfactant molecules on the nanoparticles[5]. The seminal work by Brust *et al*. has been followed by many reports on the 3-D self-assembly of alkanethiols[10–13], aromatic thiols[14–18], and alkylamines[19] on gold and silver colloidal particles. Terminally functionalized thiol molecules may also be self-assembled on colloidal nanoparticle surfaces[16,17,20–24] (Scheme 1) and this enables facile surface modification of the colloidal particles with exciting application potential. Scheme 1 illustrates the surface derivatization of colloidal gold and silver particles with 3-D self-assembled monolayers (SAMs) of ω-functionalized thiol molecules and the table in Scheme 1 lists some of the applications of the different types of terminal functionality with relevant references.

What are the possible applications of surface-derivatized nanoparticles? One of the interesting applications first investigated by Brust *et al*.[14] and thereafter studied in detail by Murray and co-workers is based on the 'nanofactory' concept (Scheme 1, Table)[14,22–24]. More specifically, the reactivities of functional groups anchored to gold colloidal particles have been investigated in some detail[22–24]. Nanoscale curvature contributes to interesting

molecular packing considerations and has been shown to play an important role in determining the S_N2 reactivity of ω-bromoalkanethiolate molecules tethered to gold nanoparticle cores with primary amines[23]. Polyfunctionalization of nanoparticles has also been demonstrated and the interesting possibilities of using such functionalized nanoparticles are discussed in detail in Templeton *et al*.[24].

Biologically important molecules may also be anchored to colloidal particle surfaces and such nanoparticles have potential applications in bio-diagnosis and immunoassays[25–27], in the assembly of nanoparticles[28–31] and as luminescent bio-conjugates for ultra-sensitive biological detection (Scheme 1, Table)[32,33]. This approach works on the basis of biomolecular recognition and is best illustrated with the well-known biotin–avidin model for ligand– receptor binding[34] (Scheme 2)[27]. Colloidal gold/silver is first derivatized with biotin molecules using thiolated biotin[27]. The advantage of using gold/silver nanoparticles in this application is

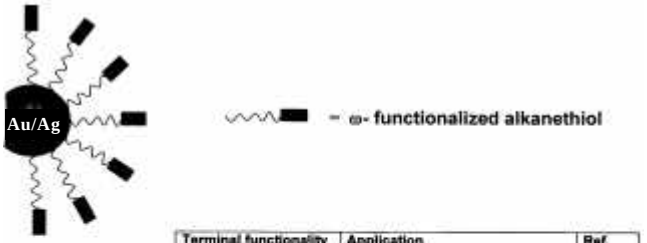

Terminal functionality	Application	Ref.
-COOH , -OH	chemical reactions such as Amide, ester formation, attachment of biomacromolecules and chromaphores	14, 22-24
Antibodies, polynucleotides	Molecular recognition/ immunoassays, detection of genetic disorders	25-33
$-NH_2$, -COOH, -SH	Colloid stabilization/ extraction and self-assembly into organized structures	16, 17, 38, 65-70, 75-79

Scheme 1. Diagram showing surface-modification of colloidal gold/ silver particles with ω-functionalized thiol molecules. The table lists some applications of surface-modified colloidal particles with corresponding references from the literature.

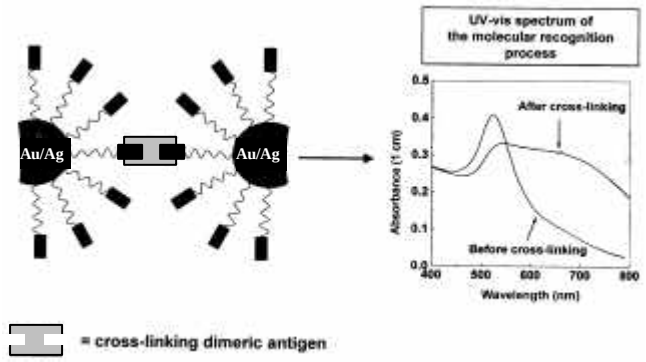

Scheme 2. Diagram showing the cross-linking of colloidal Au/Ag particles due to a molecular recognition process. Antibodies are anchored to the colloidal particle surface and cross-linking occurs via the antibody–antigen interaction, thus leading to a large change in the optical properties of the solution (see UV–vis spectrum of Au in the Scheme).

not fortuitous. Colloidal gold and silver solutions have striking colours (ruby red and bright yellow, respectively) which arise due to excitation of surface plasmon oscillations, which occurs in the visible region of the electromagnetic spectrum[35]. Thus, the optical properties are extremely sensitive to surface modification and capping with biotin molecules leads to a reduction in intensity of the plasmon resonance and a shift to larger wavelengths, a red-shift (see UV–vis spectrum for gold, Scheme 2). Thereafter if one adds the tetrameric protein, avidin, to the biotinylated gold/silver colloidal solution, high-affinity binding of the proteins to the biotin molecules occurs and leads to cross-linking of the particles (Scheme 2). A visible change in colour is observed and is a consequence of overlap of the plasmon resonances from neighbouring colloidal particles (Scheme 2)[27]. It is clear that suitably surface-modified colloidal gold and silver particles may be used for colourimetric detection of biological analytes and one interesting application already demonstrated is in the differentiation of polynucleotides with base imperfections (detection of genetic diseases)[25,26].

In addition to the above applications, surface-modification also enables stabilization of colloidal particles, especially when synthesis of the colloidal particles is carried out in an aqueous medium. Capping the colloidal particles with carboxylic acid or amine functional groups which may be ionized by controlling the solution pH leads to electrostatic stabilization of the particles in solution (Scheme 1, Table)[16,17]. Electrostatic interactions between the charged colloidal particles and suitable lipid surfaces may also be used to extract the colloidal particles from solution and organize them in thin film form. This has formed the main theme of the research activity from my lab and will be addressed next.

As an interesting aside, nanoscale curvature enables the formation of interdigitated bilayers of surfactants on colloidal particle surfaces (Scheme 3) and provides a protocol for surface modification *without the use of bifunctional molecules*. This represents an important difference between 3-D and 2-D self-assemblies where steric constraints preclude the formation of such bilayers on planar (2-D) surfaces[36]. We have shown that facile amine and carboxylic acid derivatization of colloidal silver particles may be achieved by this methodology[37,38] and have since extended it to the biotinylation of colloidal gold using alkylbiotin molecules (Scheme 3)[39]. This approach has been used for the stabilization of magnetic fluids recently[40].

Self-assembly of surface-derivatized colloidal particles

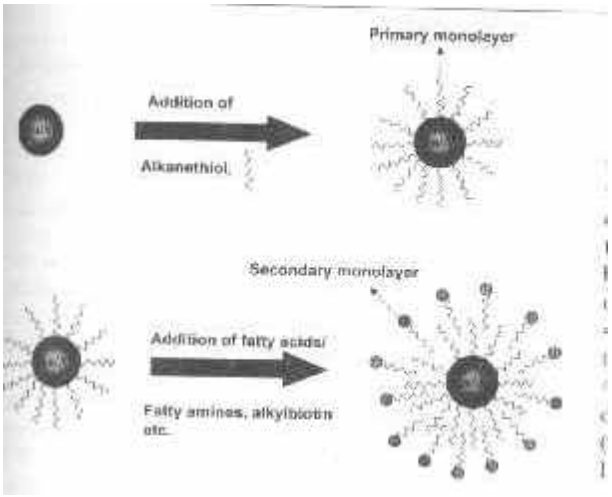

Scheme 3. Surface modification of colloidal nanoparticles via interdigitated bilayer formation. The various steps in the surface-modification procedure are illustrated.

Different approaches have been investigated for the organization of nanoparticles in thin film form. Some of the more prominent nanoparticle film formation methods include, (1) self-assembly by simple solvent evaporation[5,12,41–43]; (2) covalent attachment to suitably modified surfaces[44–49]; (3) using molecular recognition events for self-assembly[31]; and (4) organization at the air–water (using hydrophobized colloidal particles)[50–52] and water–organic solution interfaces[53,54] and formation thereafter of superlattice films by the Langmuir–Blodgett (LB) technique. As mentioned above, we have primarily concentrated on using electrostatic interactions between charged colloidal particles (the charging accomplished by derivatization with ionizable carboxylic acid and amine functional groups) and ionizable lipid molecules in film form to organize the colloidal particles. Electrostatic interactions, which have long been known to play an important role in biological and chemical processes[55] have only recently been investigated for the growth of multilayer polyelectrolyte[56,57] and nanoparticle–polyelectrolyte films[58] as well as micron-sized objects[59].

Two techniques have been investigated in some detail in this laboratory for the growth of thin nanoparticle films and are based on (1) electrostatic self-assembly at the air–water interface with charged Langmuir monolayers, and (2) electrostatically controlled diffusion into thermally evaporated fatty lipid films.

Electrostatic complexation of colloidal nanoparticles with charged Langmuir monolayers at the air–water interface

The air–water interface has long been recognized to be an excellent medium for the organization of inorganic cations using charged amphiphilic monolayers (Langmuir monolayers)[60]. This approach has now been extended to the organization of large inorganic anions[61–63] and biological macromolecules as well[64,65]. It is clear from the above that electrostatic interaction between the ions/macromolecules in solution and charged lipid Langmuir monolayers drives the organization at the air–water interface. Proceeding in this spirit, we have demonstrated that colloidal nanoparticles, which may be charged using surface-bound ionizable groups, may also be electrostatically bound to charged Langmuir monolayers[36,38,66–71]. Moreover, the nanoparticle organizates can be transferred onto suitable substrates and superlattice structures formed by the elegant LB technique[36,38,66–71], as illustrated in Scheme 4. As an example, the immobilization of carboxylic acid derivatized silver colloidal particles at octadecylamine (ODA) Langmuir monolayer surfaces and formation of LB films is described.

Silver colloidal solution was prepared by borohydride reduction of Ag_2SO_4 solution and the resulting particles capped with a bifunctional molecule, 4-carboxythiophenol (4-CTP)[17,67]. The 4-CTP molecules chemisorb on the silver colloidal particle surface, this process derivatizing the surface with carboxylic acid groups. Under basic conditions the carboxylic acid groups are ionized and this leads to long-term stability of the colloidal solutions[17]. ODA molecules were dispersed on the surface of the colloidal solution held at different pH values and complexation of the colloidal particles with the ODA Langmuir monolayer followed as a function of time of spreading the monolayer. This is conveniently done by measuring the pressure–area (p–A) iso-

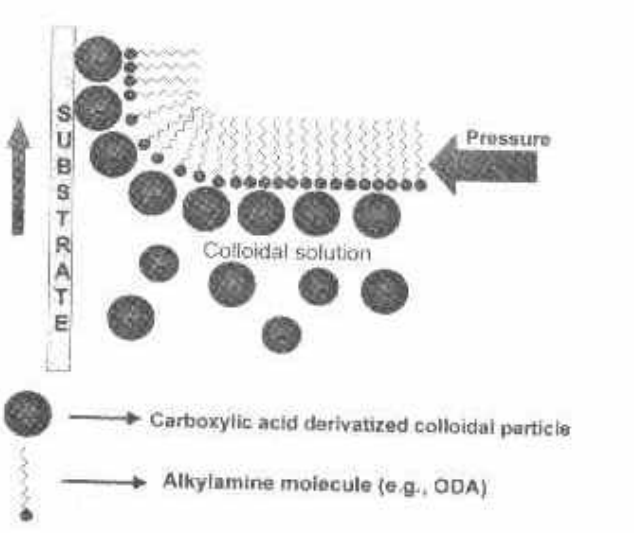

Scheme 4. Diagram showing the electrostatic immobilization of carboxylic acid derivatized colloidal nanoparticles at the air–water interface with positively charged ODA molecules and transfer thereafter of the nanoparticle monolayer onto suitable substrates by the LB technique.

therms[72] with time and is shown for the ODA–silver colloidal particle complexation process in Figure 1. The solid lines refer to the isotherm measured immediately after spreading the ODA monolayer (t = 0 min) and the dashed lines are the isotherms measured 90 min after spreading. It is clear that the area/ODA molecule increases with time for the Langmuir monolayer of silver colloidal solution at pH = 9 (Figure 1 *a*) and also that no expansion of the monolayer is observed when the colloidal solution subphase is at pH = 12 (Figure 1 *b*). At pH = 9, both the ODA molecules and the carboxylic acid groups on the colloidal particle surface are fully ionized, leading to maximum attractive electrostatic interaction and a large increase in the Langmuir monolayer area with time (Figure 1 *a*). On the other hand at pH = 12, the ODA molecules are un-ionized and in the absence of the electrostatic driving force, no complexation occurs and the p–A isotherms are relatively unchanged with time (Figure 1 *b*). The complexation process is quite slow and equilibrium nanoparticle density at the air–water interface is achieved only after 12 h of spreading the Langmuir monolayer[68]. It is clear from Figure 1 that electrostatic interactions play a crucial role in the complexation process. By simple variation of the colloidal solution pH, it is possible to modulate the electrostatic interaction between the colloidal particles and the Langmuir monolayer and thus vary the nanoparticle concentration at the air–water interface. This has been demonstrated for a number of other colloidal particle systems such as gold[66,69] and CdS quantum dots[71] as well.

The formation of superlattice films of the colloidal particles organized at the air–water interface was effected by the LB technique. This is a simple (and versatile) technique wherein a solid support is slowly immersed in the Langmuir monolayer covered trough and withdrawn (Scheme 4)[60]. Each immersion cycle enables transfer of a bilayer of the Langmuir monolayer and in this fashion, superlattices of the colloidal silver particles were grown on different substrates and analysed using a host of techniques. Figure 2 shows a plot of the quartz crystal microgravimetry (QCM)[73] mass uptake measured as a function of the number of monolayers of silver colloidal particles in the film. These measurements were performed for films grown from colloidal solution subphases held at different pH values. It is observed from Figure 2 that the mass uptake increases linearly with increasing film thickness (number of monolayers transferred) indicating that the integrity (in terms of particle density) of the nanoparticle assembly at the air–water interface is maintained on transfer to the solid substrate. This is an extremely important requirement for commercial application of the nanoparticle thin films. The mass uptake is considerably larger for the pH = 9 case, indicating that the silver particle density in the films is higher than at pH = 12. Figure 3 *a* shows a plot of the UV–vis spectra recorded from LB films of the silver particles transferred onto quartz substrates from the pH = 9 colloidal subphase. A strong resonance is seen at ca. 460 nm and is due to excitation of surface plasmon oscillations[35]. The inset in Figure 3 *a* show plots of the plasmon resonance intensity as a function of the number of monolayers in the film for LB films grown from both the pH = 9 and pH = 12 colloidal subphases. It is seen that the intensity of the plasmon resonance increases linearly with the number of monolayers transferred at pH = 9 while the silver particles were below detection limits for the pH = 12 case. The mass uptake observed in the QCM studies at pH = 12 (Figure 2) is thus attributed to transfer of the ODA monolayer alone without the colloidal silver particles.

An estimate of the thickness of the monolayers of the colloidal particles was made using optical interferometry. The film thickness as a function of the number of monolayers transferred from the pH = 9 subphase is shown in Figure 3 *b*. It is seen that a linear increase in film thickness occurs indicating that in addition to the cluster density in

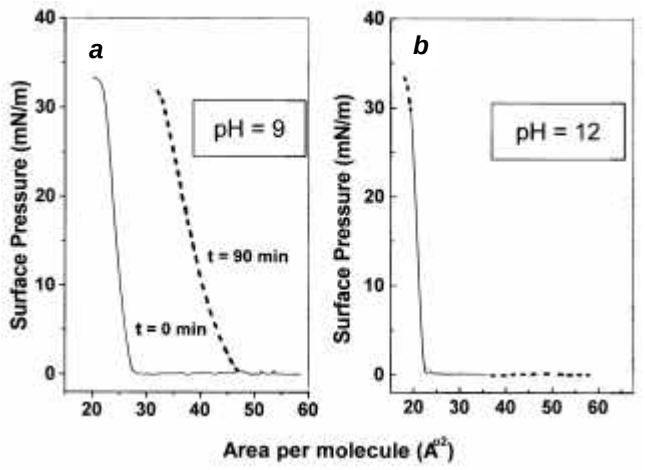

Figure 1. p–A isotherms of ODA monolayers spread on carboxylic acid derivatized colloidal silver solution at (***a***) pH = 9 and (***b***) pH = 12, recorded as a function of time of spreading the monolayer (solid line, t = 0 min and dashed line, t = 90 min).

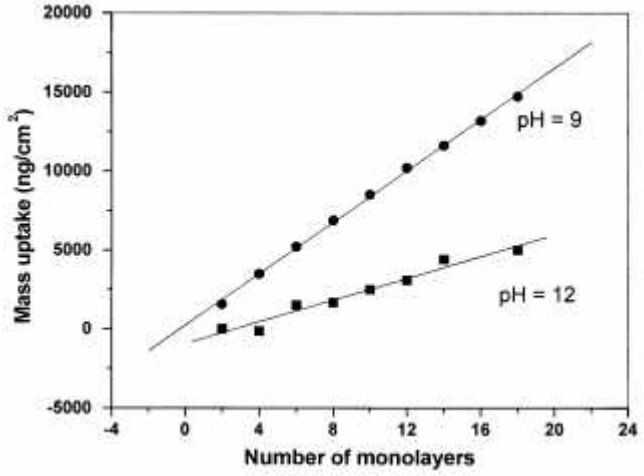

Figure 2. QCM mass uptake recorded as a function of number of monolayers of carboxylic acid silver colloidal particles transferred from different pH subphases onto the quartz crystal. The solid lines are nonlinear least squares fits to the QCM data.

the films being constant during each transfer cycle number, the film grows in an essentially lamellar fashion. The slope of the curve in Figure 3 *b* yields a thickness increment to the film of ca. 105 Å/monolayer. The ODA bilayer thickness is ca. 50 Å from which a cluster diameter of 56 Å is calculated. This value is marginally less than the value of 70 Å obtained by an electron microscopy analysis of the colloidal solution and together with infrared measurements, indicates some disorder in the chains.

To conclude this section, it has been shown that surface-modified colloidal particles may be electrostatically self-assembled at the air–water interface and that lamellar superlattice films can be grown by the LB technique. The electrostatic interaction (and thereby, the nanoparticle density in the films) between the colloidal particles and the charged Langmuir monolayer may be controlled by simple variation of the colloidal solution pH. This technique shows promise for growing hetero-colloidal particle superlattice structures (such as alternating gold and silver nanoparticle layers)[74] which are currently realized using self-assembly of nanoparticles with a dithiol cross-linking molecule[49].

Formation of colloidal nanoparticle–fatty lipid composites by electrostatically controlled diffusion process

The origin of this approach towards the assembly of surface-modified colloidal particles may be traced to the early work carried out in this lab on the spontaneous self-organization of thermally evaporated fatty acid films on immersion in a suitable electrolyte solution[75]. It was observed that exchange of the carboxylic acid protons in the fatty acid film with cations from the solution leads to organization of the film into a *c*-axis oriented structure, similar to that obtained by the LB technique. Carrying this technique a little further, we have demonstrated that charged colloidal particles may also be incorporated into thermally evaporated fatty lipid films via selective electrostatic interactions[37,76–80].

Scheme 5 illustrates the methodology used in this approach. Negatively charged colloidal particles (charging accomplished by ionizing surface-bound carboxylic acid groups, for example) are incorporated into thermally evaporated fatty amine films, such as ODA, by simple immersion of the films in the colloidal solution. Under appropriate conditions of the solution pH, the electrostatic interaction between the negatively charged colloidal particles and positively charged ODA matrix can be maximized to drive the diffusion of the colloidal particles into the films (Scheme 5). This results in a nanocomposite film and in the case of diffusion of colloidal gold and silver particles, the cluster incorporation can be observed by the unaided eye in the form of colouration of the film, the intensity of which increases with time.

The process of cluster diffusion into thermally evaporated fatty amine films is easily studied using QCM. Figure 4 shows the mass uptake of a 500 Å thick ODA during immersion in carboxylic acid derivatized colloidal gold solutions held at different pH values. The size of the gold particles in this experiment is 130 Å, the synthesis and capping of which are described in detail in ref. 80. It is observed that the cluster density in the films is much higher in the case of films grown from pH = 7 solution than those grown from higher and lower pH solutions. This may be explained in terms of the degree of ionization of the colloidal surface-bound carboxylic acid groups and the amine groups in the thermally evaporated film which is modulated by varying the solution pH and clearly indicates that electrostatic interactions drive the cluster diffusion into the lipid matrix.

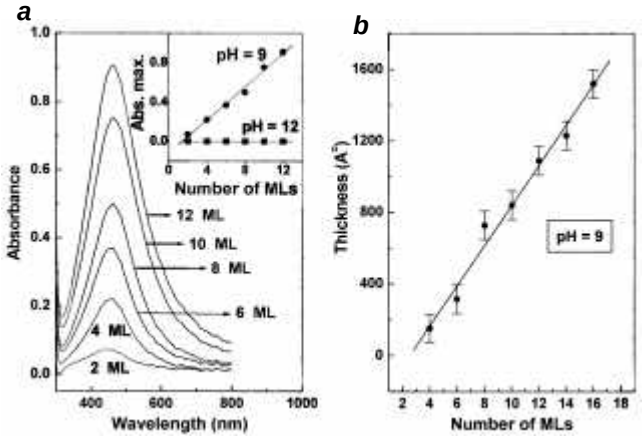

Figure 3. ***a***, UV–vis spectra recorded from the silver colloidal particle LB films as a function of thickness of the films. The number of monolayers (ML) of the colloidal particles transferred onto quartz is indicated next to the respective curves. The inset shows a plot of the intensity of the plasmon resonance with thickness of silver particle LB film for the films grown from the pH = 9 and 12 subphases; ***b***, Thickness of LB films of colloidal silver particles estimated from optical interferometry measurements as a function of number of

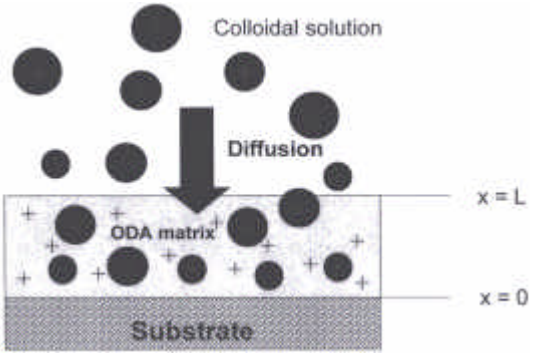

Scheme 5. Diagram showing the diffusion of carboxylic acid derivatized colloidal particles into thermally evaporated ODA films by a simple beaker-based immersion process.

Figure 5 shows the QCM mass uptake kinetics for a 500 Å thick ODA film immersed in colloidal gold solutions of different particle sizes. It is observed that the cluster diffusion is extremely rapid in the case of the smallest gold particles (20 Å diameter) and slows down as the particle size increases. In order to quantify the cluster movement into the thermally evaporated lipid films, the QCM mass uptake data was analysed in terms of a 1-D diffusion model. The mathematical details of the model and its connection to the QCM mass uptake kinetics have been dealt with in detail in refs 77, 79, 80 and will not be dealt with here. The parameters of interest are the cluster diffusivity and the concentration of the colloidal particles at the film-solution interface (at $x = L$, Scheme 5). These parameters were left free in a nonlinear least squares fit to the QCM data in terms of the 1-D diffusion model and are listed in Table 1. These parameters have been determined from an analysis of the QCM data shown in Figures 4 and 5 where the solution pH (and consequently the magnitude of the electrostatic interaction) and the gold particle size have been varied. The main features of the analysis are that the smaller colloidal particles do indeed have larger diffusivities (D, Table 1), as was evident from the QCM mass uptake data shown in Figure 5, and that there is a large increase in the colloidal particle concentration (C_0, Table 1) at the film–colloidal solution interface. In fact, the cluster concentration at the interface is nearly 3–5 orders of magnitude greater than the nominal cluster concentration in the bulk of the colloidal solution. This is an interesting result and is similar to the large enhancement of the counterion concentration observed for small inorganic ions complexed with charged Langmuir monolayers[81]. Attempts to understand the complexation of large ions with charged surfaces in terms of a Poisson–Boltzmann–Stern formalism are currently in progress[82,83] and there is scope for further theoretical input here.

The variation in the equilibrium colloidal particle volume fraction with solution pH was investigated for 500 Å thick ODA films immersed in the gold colloidal solutions of different sizes (Figure 6). The variation in pH at which maximum cluster incorporation occurs as well as the width

Table 1. Parameters based on a 1-D diffusion model obtained from fits to the QCM mass uptake data of gold colloidal particles in thermally evaporated octadecylamine films

Experiment	$C_0 \times 10^{18}$ (clusters/cm^3)	$D \times 10^4$ (Å^2/h)
A. Film thickness = 500 Å (950 Å)[a] *Sol 1 (130 Å size Au)*		
pH = 5.2	0.08	1.3
pH = 6.0	0.15	1.2
pH = 7.0	0.21	1.2
pH = 11.2	0.07	0.9
B. Hydrosol pH = 7.0 Sol 1 (130 Å size Au)		
Thickness = 250 Å (520 Å)[a]	0.25	0.5
Thickness = 500 Å (950 Å)[a]	0.21	1.2
Thickness = 1000 Å (1900 Å)[a]	0.20	1.8
C. Film thickness = 500 Å		
Sol 1/130 Å gold (950 Å, pH = 7)[a]	0.21	1.2
Sol 2/40 Å gold (1100 Å, pH = 8.5)[a]	10.37	2.5
Sol 3/20 Å gold (1300 Å, pH = 8.5)[a]	400	6.4

[a]The numbers in parentheses are the values of the film thickness used in the 1-D diffusion calculations.

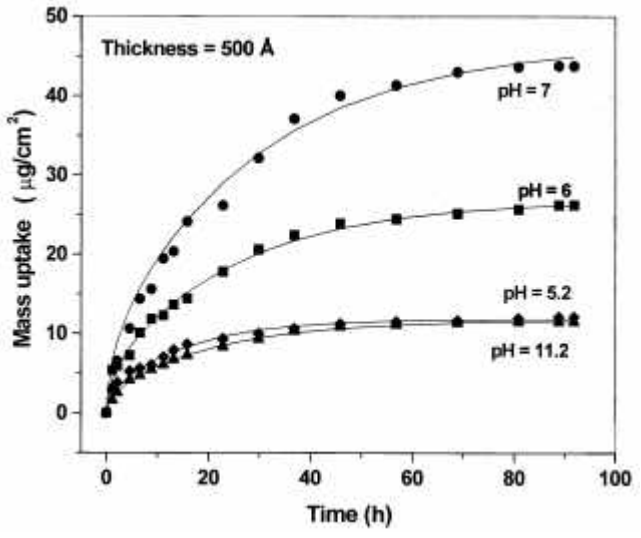

Figure 4. QCM mass uptake kinetics data of 500 Å thick ODA films immersed in carboxylic acid derivatized colloidal gold solutions held at different pH values (the values are indicated next to the corresponding curves). The solid lines are based on a 1-D diffusion analysis of the QCM data.

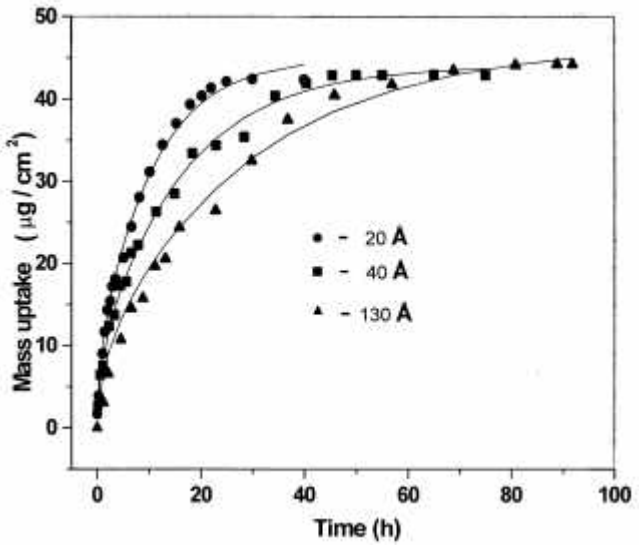

Figure 5. QCM mass uptake kinetics data of 500 Å thick ODA films immersed in carboxylic acid derivatized colloidal gold solutions of different particles sizes. The solid lines are based on a 1-D diffusion analysis of the QCM data.

of the curves (the data were fit to Lorentzians) with particle size are shown in the inset. It is seen that the pH at which maximum cluster uptake occurs is a strong function of the particle size, or in other words, the curvature of the particles. Increasing surface curvature, as would occur for the small gold particles, leads to reduced interaction between the surface-bound carboxylic acid groups (Figure 6 and inset) and affects the ionization constant[84]. We have already seen how surface curvature enables formation of interdigitated bilayers on colloidal particles (Scheme 3) and this is another instance of the role played by nanoscale curvature affecting, in this case, the reactivity of terminal functional groups.

Figure 7 shows a parallel UV–vis study of 130 Å gold colloidal particle diffusion into 500 Å thick ODA films as a function of time of immersion. Figure 7 *a* shows the spectra recorded for the films *ex-situ* while Figure 7 *b* shows the spectra recorded in the colloidal solution. There is a steady increase in the plasmon resonance of gold with time (which occurs at ca. 575 nm for the films in air and 530 nm for the films in solution) and indicates that the particle density increases in the films. What is interesting is that values of the plasmon resonance wavelengths are different in the films in air and in solution. This indicates that the films in solution swell (this also establishes a mechanism for cluster diffusion into the films) and as a consequence, the effective refractive index of the medium in which the particles are embedded is less than that of the film in air. This shift may thus be rationalized in terms of an effective medium Mie theory[35].

The diffusion of 130 Å gold colloidal particles into a 500 Å thick ODA film was also followed with Fourier Transform Infrared (FTIR) Spectroscopy and the spectra obtained with time are shown in Figure 8. The methylene antisymmetric and symmetric vibrational modes at 2920 and 2850 cm^{-1} are shown in Figure 8 *a*. It is observed that the intensity of these peaks reduces with time but remains at the same frequencies. This indicates that the orientation of the hydrocarbon chains is randomized as the particles diffuse into the ODA matrix. The $–NH_2$ antisymmetric vibration at ca. 3300 cm^{-1} is shown in the inset of Figure 8 *a* and the intensity of this peak steadily decreases with time without a shift.

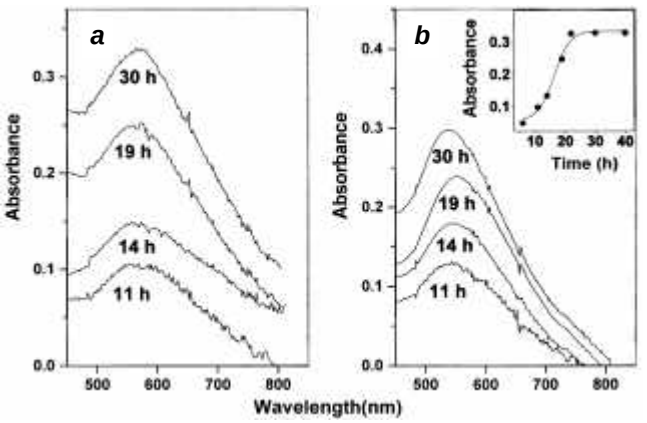

Figure 7. ***a***, UV–vis spectra measured *ex-situ* of 130 Å colloidal gold–ODA composite films as a function of time of immersion of the ODA film in the colloidal solution (the time of immersion is indicated next to the corresponding curves); ***b***, UV–vis spectra measured *in-situ* of 130 Å colloidal gold–ODA composite films as a function of time of immersion of the ODA film in the colloidal solution (the time of immersion is indicated next to the corresponding curves). The inset shows a plot of the variation of the surface plasmon resonance intensity with time of immersion of the films shown in the main part of Figure 7 *b*.

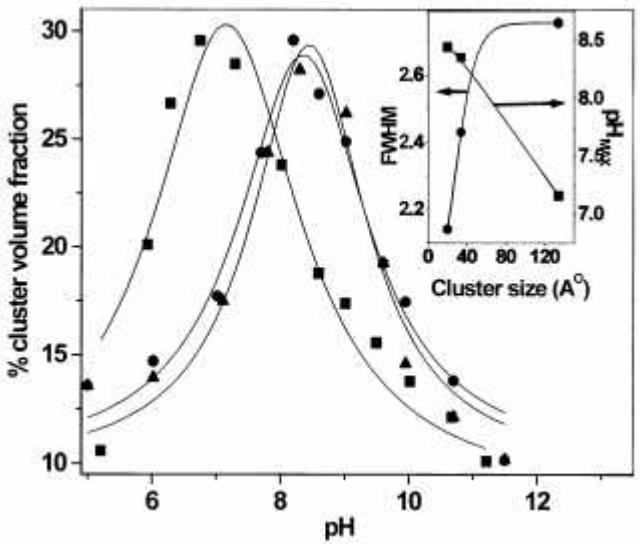

Figure 6. Equilibrium percentage volume fractions of colloidal gold particles of different sizes incorporated into 500 Å thick ODA films as a function of colloidal solution pH. These values were estimated from QCM measurements. The inset gives a plot of the pH at which maximum particle uptake occurs and the width of the fitted Lorentzian curves as a function of colloidal particle size.

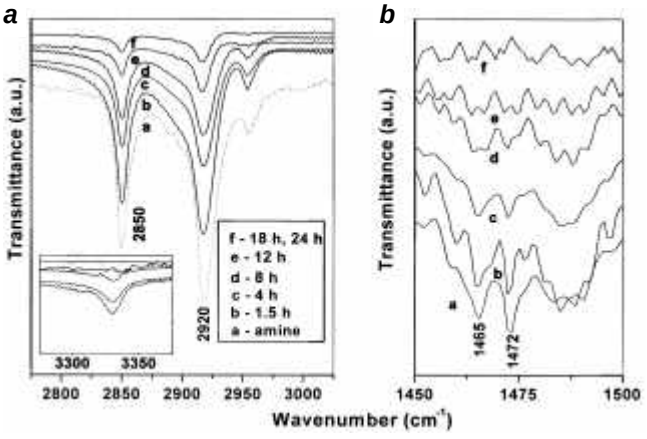

Figure 8. FTIR spectra recorded as a function of time of immersion of 500 Å thick ODA films in 130 Å colloidal gold solution in the range of (***a***) the methylene antisymmetric and symmetric vibrations (inset shows the corresponding spectra in the amine antisymmetric vibration mode region) and (***b***) the methylene scissoring vibrations.

Thus, the interaction between the colloidal particles and the ODA matrix is weak and in this sense, differs from salt formation in amines where a large shift in this vibrational mode has been observed[85]. Figure 8 *b* shows the methylene scissoring bands at 1465 and 1472 cm^{-1}. The splitting of these bands is a sensitive indicator of the crystalline environment of the hydrocarbon chains[86]. It is seen from the figure that the splitting in the bands decreases as the cluster density in the films increases, suggesting decrease in the packing density of the ODA hydrocarbon chains. The FTIR data shown in Figure 8 are consistent with a randomization of the ODA molecules due to electrostatic coordination with the negatively charged carboxylic acid groups on the colloidal particle surface. This leads to the formation of an ODA surfactant sheath around the particles and has been used to render the particles hydrophobic and thus soluble in non-polar organic solvents[87].

Thus, it has been shown that electrostatically controlled diffusion of colloidal nanoparticles can be achieved by a simple beaker-based approach and that the composition of the nanocomposite films can be tailored by variation of the colloidal solution pH. This method has been successfully applied to silver nanoparticles[79] and quantum dot CdS (ref. 77) colloidal particles as well and has been extended to the encapsulation of biomacromolecules such as proteins very recently[88,89]. There is much scope for application of this technique in assembling biological molecules and this is currently being explored in our laboratory.

Conclusions

A very brief overview of the recent developments in the area of self-assembly of colloidal nanoparticles has been attempted and the results of the research efforts from my laboratory on the use of electrostatic interactions in the formation of nanoparticle thin films addressed in some detail. Some of the open questions in this area have been discussed. Possible applications of surface-modified colloidal particles currently being pursued by different research groups have been mentioned.

1. Feynman, R. P., in a lecture delivered at the American Physical Society Meeting, 1959.
2. Henglein, A., *Chem. Rev.*, 1989, **89**, 1861.
3. DeHeer, W. A., *Rev. Mod. Phys.*, 1993, **65**, 611.
4. The bottom-up method is a relatively new alternative to the 'top-down' technique currently in vogue in the electronics industry wherein nanoscale structures are carved out of bulk objects. Lithographic and ion-beam etching techniques are used extensively in the top-down approach.
5. Brust, M., Walker, M., Bethell, D., Schiffrin, D. J. and Whyman, R., *J. Chem. Soc., Chem. Commun.*, 1994, 801.
6. Nuzzo, R. G. and Allara, D. L., *J. Am. Chem. Soc.*, 1983, **105**, 4481.
7. Freeman, T. L., Evans, S. D. and Ulman, S. D., *Langmuir*, 1995, **11**, 4411.
8. Sagiv, J., *J. Am. Chem. Soc.*, 1980, **102**, 92.
9. Maoz, R. and Sagiv, J., *J. Colloid Interface Sci.*, 1984, **100**, 465.
10. Terrill, R. H., Postlewaithe, T. A., Chen, C., Poon, C., Terzis, A., Chen, A., Hutchinson, J. E., Clark, M. R., Wignall, G., Londono, J. D., Superfine, R., Falvo, M., Johnson Jr., C. S., Samulski, E. T. and Murray, R. W., *J. Am. Chem. Soc.*, 1995, **117**, 12537.
11. Leff, D. V., Ohara, P. C., Heath, J. C. and Gelbart, W. M., *J. Phys. Chem.*, 1995, **99**, 7036.
12. Vijaya Sarathy, K., Raina, G., Yadav, R. T., Kulkarni, G. U. and Rao, C. N. R., *J. Phys. Chem. B*, 1997, **101**, 9876.
13. Porter, L. A., Ji, D., Westcott, S. L., Graupe, M., Czernuszewicz, R. S., Halas, N. J. and Lee, T. R., *Langmuir*, 1998, **14**, 7378.
14. Brust, M., Fink, J., Bethell, D., Schiffrin, D. J. and Kiely, C., *J. Chem. Soc. Chem. Commun.*, 1995, 1655.
15. Johnson, S. R., Evans, S. D., Mahon, S. W. and Ulman, A., *Langmuir*, 1997, **13**, 51.
16. Mayya, K. S., Patil, V. and Sastry, M., *Langmuir*, 1997, **13**, 3944.
17. Sastry, M., Mayya, K. S. and Bandyopadhyay, K., *Coll. Surf. A*, 1997, **127**, 221.
18. Chen, S. and Murray, R. W., *Langmuir*, 1999, **15**, 682.
19. Leff, D. V., Brandt, L. and Heath, J. R., *Langmuir*, 1996, **12**, 4723.
20. Weisbecker, C. S., Merritt, M. V. and Whitesides, G. M., *Langmuir*, 1996, **12**, 3763.
21. Evans, S. D., Johnson, S. R., Ringsdorf, H., Williams, L. M. and Wolf, H., *Langmuir*, 1998, **14**, 6436.
22. Ingram, R. S., Hostetler, M. J. and Murray, R. W., *J. Am. Chem. Soc.*, 1997, **119**, 9175.
23. Templeton, A. C., Hostetler, M. J., Kraft, C. T. and Murray, R. W., *J. Am. Chem. Soc.*, 1998, **120**, 1906.
24. Templeton, A. C., Hostetler, M. J., Warmoth, E. K., Chen, S., Hartshorn, C. M., Krishnamurthy, V. M., Forbes, D. E. and Murray, R.W., *J. Am. Chem. Soc.*, 1998, **120**, 4845.
25. Elghanian, R., Storhoff, J. J., Mucic, R. C., Letsinger, R. L. and Mirkin, C., *Science*, 1997, **277**, 1078.
26. Storhoff, J. J., Elghanian, R., Mucic, R. C., Mirkin, C. A. and Letsinger, R. L., *J. Am. Chem. Soc.*, 1998, **120**, 1959.
27. Sastry, M., Lala, N., Patil, V., Chavan, S. P. and Chittiboyina, A. G., *Langmuir*, 1998, **14**, 4138.
28. Mirkin, C. A., Letsinger, R. L., Mucic, R. C. and Storhoff, J. J., *Nature*, 1996, **382**, 607.
29. Mucic, R. C., Storhoff, J. J., Mirkin, C. A. and Letsinger, R. L., *J. Am. Chem. Soc.*, 1998, **120**, 12674.
30. Alivisatos, A. P., Johnsson, K. P., Peng, X., Wilson, T. E., Loweth, C. J., Brunchez Jr., M. P. and Schultz, P. G., *Nature*, 1996, **382**, 609.
31. Li, M., Wong, K. K. W. and Mann, S., *Chem. Mater.*, 1999, **11**, 23.
32. Chan, W. C. W. and Nie, S., *Science*, 1998, **281**, 2016.
33. Bruchez Jr., M., Moronne, M., Gin, P., Weiss, S. and Alivisatos, A. P., *Science*, 1998, **281**, 2013.
34. Blankenburg, R., Meller, P., Ringsdorff, H. and Salesse, C., *Biochemistry*, 1989, **28**, 8214.
35. Mulvaney, P., *Langmuir*, 1996, **12**, 788.
36. Patil, V., Mayya, K. S., Pradhan, S. D. and Sastry, M., *J. Am. Chem. Soc.*, 1997, **119**, 9281.
37. Patil, V. and Sastry, M., *Langmuir*, 1998, **14**, 2707.
38. Sastry, M., Mayya, K. S. and Patil, V., *Langmuir*, 1998, **14**, 5921.
39. Lala, N., Chittiboyina, A. G., Chavan, S. P. and Sastry, M., Paper presented at the 5th International Symposium on Bio-Organic Chemistry, Pune, 30 January–4 February 2000.
40. Shen, L., Laibinis, P. E. and Hatton, T. A., *Langmuir*, 1999, **15**, 447.
41. Brinker, C. J., Lu, Y., Sellinger, A. and Fan, H., *Adv. Mater.*, 1999, **11**, 579.
42. Wang, Z. L., *Adv. Mater.*, 1998, **10**, 13.
43. Connolly, S., Fullam, S., Korgel, B. and Fitzamurice, D., *J. Am.*

Chem. Soc., 1998, **120**, 2969.
44. Colvin, V. L., Goldstein, A. N. and Alivisatos, A. P., *J. Am. Chem. Soc.*,1992, **114**, 5221.
45. Chumanov, G., Sokolov, K., Gregory, B. W. and Cotton, T. M., *J. Phys. Chem.*, 1995, **99**, 9466.
46. Grabar, K. C., Smith, P. C., Musick, M. D., Davis, J. A., Walter, D. G., Jackson, M. A., Guthrie, A. P. and Natan, M. J., *J. Am. Chem. Soc.*, 1996, **118**, 1148.
47. Bandyopadhyay, K., Patil, V., Vijayamohanan, K. and Sastry, M., *Langmuir*, 1997, **13**, 5244.
48. Garcia, M. E., Baker, L. A. and Crooks, R. M., *Anal. Chem.*, 1999, **71**, 256.
49. Sarathy, K. V., Thomas, J. P., Kulkarni, G. U. and Rao, C. N. R., *J. Phys. Chem. B*, 1999, **103**, 399.
50. Fendler, J. H. and Meldrum, F., *Adv. Mater.*, 1995, **7**, 607 and references therein.
51. Sastry, M., Patil, V., Mayya, K. S., Paranjape, D. V., Singh, P. and Sainkar, S. R., *Thin Solid Films*, 1998, **324**, 239.
52. Sastry, M., Patil, V. and Gole, A., *Langmuir*, 2000 (communicated).
53. Mayya, K. S. and Sastry, M., *Langmuir*, 1999, **15**, 1902.
54. Mayya, K. S. and Sastry, M. (unpublished results).
55. Honig, B. and Nicholls, A., *Science*, 1995, **268**, 1144.
56. Taguchi, Y., Kimura, R., Azumi, R., Tachibana, H., Koshizaki, N., Shimomura, M., Momozawa, N., Sakai, H., Abe, M. and Matsumoto, M., *Langmuir*, 1998, **14**, 6550.
57. Lvov, Y., Ariga, K., Ichinose, I. and Kunitake, T., *J. Am. Chem. Soc.*, 1995, **117**, 6117.
58. Caruso, F., Lichtenfeld, H., Giersig, M. and Mohwald, H., *J. Am. Chem. Soc.*, 1998, **120**, 8523.
59. Tien, J., Terfort, A. and Whitesides, G. M., *Langmuir*, 1997, **13**, 5349.
60. Ulman, A., *An Introduction to Ultrathin Organic Films: From Langmuir–Blodgett to Self-Assembly*, Academic Press, San Diego, CA, 1991. This book introduces the essential concepts behind
organization of monolayers of amphiphiles (Langmuir monolayers) on the surface of water and the methodology for formation of built-up LB films.
61. Ganguly, P., Paranjape, D. V. and Sastry, M., *J. Am. Chem. Soc.*, 1993, **115**, 793.
62. Ganguly, P., Paranjape, D. V., Patil, K. R., Sastry, M. and Rondelez, F., *Langmuir*, 1997, **13**, 5440.
63. Clemente-Leon, M., Mingotaud, C., Agricole, B., Gomez-Garcia, C. J., Coronado, E. and Delhaes, P., *Angew. Chem. Int. Ed. Engl.*, 1997, **36**, 1114.
64. Riccio, A., Lanzi, M., Antolini, F., De Nitti, C., Tavani, C. and Nicolini, C., *Langmuir*, 1996, **12**, 1545.
65. Raedler, U., Heiz, C., Luigi, P. and Tampe, R., *Langmuir*, 1998, **14**, 6620.
66. Mayya, K. S., Patil, V. and Sastry, M., *Langmuir*, 1997, **13**, 2575.
67. Sastry, M., Mayya, K. S., Patil, V., Paranjape, D. V. and Hegde, S. G., *J. Phys. Chem. B*, 1997, **101**, 4954.
68. Mayya, K. S. and Sastry, M., *J. Phys. Chem. B*, 1997, **101**, 9790.
69. Mayya, K. S., Patil, V. and Sastry, M., *J. Chem. Soc., Faraday Trans.*, 1997, **93**, 3377.
70. Mayya, K. S. and Sastry, M., *Langmuir*, 1998, **14**, 74.
71. Mayya, K. S., Patil, V., Kumar, M. and Sastry, M., *Thin Solid Films*, 1998, **312**, 308.
72. π-*A* isotherms measure the change in surface tension of the surfactant (ODA–silver colloidal particle complex in this case) covered water surface as a function of area of the surfactant monolayer. Increase in the area of the surfactant molecules due to complexation of ions may readily be observed.
73. In QCM, the change in the resonance frequency of a piezoelectric quartz crystal on deposition of material on its surface is used to estimate the mass of the material. It is extremely sensitive to minute mass changes and the instrument used in these studies had a mass resolution of ca. 12 ng/cm^2.
74. Sastry, M. and Mayya, K. S., *J. Nano. Res.*, 2000 (in press).
75. Ganguly, P., Pal, S., Sastry, M. and Shashikala, M. N., *Langmuir*, 1995, **11**, 1078.
76. Sastry, M., Patil, V. and Mayya, K. S., *Langmuir*, 1997, **13**, 4490.
77. Patil, V. and Sastry, M., *J. Chem. Soc. Faraday Trans.*, 1997, **93**, 4347.
78. Patil, V. and Sastry, M., *Langmuir*, 1997, **13**, 5511.
79. Sastry, M., Patil, V. and Sainkar, S. R., *J. Phys. Chem. B*, 1998, **102**, 1404.
80. Patil, V., Malvankar, R. B. and Sastry, M., 1999, *Langmuir*, **15**, 8197.
81. Israelachvili, J. N., *Intermolecular and Surface Forces*, Academic Press, San Diego, CA, 1991, 2nd edn.
82. Borukhov, I., Andelman, D. and Orland, H., *Phys. Rev. Lett.*, 1997, **79**, 435.
83. Cuvillier, N. and Rondelez, F., *Thin Solid Films*, 1998, **327–329**, 19.
84. Gole, A., Sathivel, C., Lachke, A. and Sastry, M., *J. Chromatogr. A*, 1999, **848**, 485.
85. Bardosova, M., Tregold, R. H. and Ali-Adib, Z., *Langmuir*, 1995, **11**, 1273.
86. Rabolt, J. F., Burns, F. C., Schlotter, N. E. and Swalen, J. D., *J. Chem. Phys.*, 1983, **78**, 946.
87. Patil, V. and Sastry, M., *Langmuir*, 2000, **16**, 2207.
88. Gole, A., Dash, C. V., Rao, M. and Sastry, M., *J. Chem. Soc., Chem. Commun.*, 2000, 297.
89. Gole, A. and Sastry, M., Paper presented at the 5th International Symposium on Bio-Organic Chemistry, Pune, 30 January–4 February 2000.

ACKNOWLEDGEMENTS. I thank my students, Drs K. S. Mayya and Vijaya Patil who contributed significantly to this work, the major portion of which formed the basis of their Ph D dissertations. I would like to acknowledge Dr P. Ganguly, Head, Physical and Materials Chemistry Division, NCL, Pune, for starting me out in this area and being a constant source of encouragement. This work was made possible through a Young Scientist Award grant to me from the Council of Scientific and Industrial Research (CSIR), Govt of India, and is gratefully acknowledged.
Received 4 January 2000; revised accepted 6 March 2000